

Studies of High-Speed Metal–Semiconductor–Metal Photodetector with a GaAs/AlGaAs/GaAs Heterostructure

Jian Lu, R. Surridge, G. Pakulski, H. van Driel, and J. M. Xu, *Senior Member, IEEE*

Abstract—A GaAs/AlGaAs/GaAs heterostructure metal–semiconductor–metal photodetector (HMSM), with an active area of $100 \times 100 \mu\text{m}^2$, has been developed and studied. The measured rise time of the device is 30 ps. More importantly, the measured fall time is as short as 23 ps, which is the shortest reported for an MSM photodetector of similar size. The observed ultrafast response is attributed to the reduction of both the carrier transit time and the device capacitance due to the incorporation of the AlGaAs barrier layer. The HMSM is found to have a smaller saturation capacitance and saturates at a much lower bias voltage in comparison with the conventional MSM photodetector (CMSM). At a bias of 10 V, the full width at half maximum (FWHM) of the temporal response of the HMSM is more than 20% smaller than that of the CMSM. In addition, it is found that the peak impulse response for the HMSM is substantially larger than that of the CMSM under the same operation condition. Two-dimensional simulations and equivalent circuit analysis have been carried out to interpret the observed phenomena and to provide insight into the underlying physics.

I. INTRODUCTION

THE MSM interdigital photodetector has attracted a great deal of attention for application in optical communication and interconnects because of its simple processing requirement and high performance [1]–[4]. Based on an interdigitated Schottky contact structure, the MSM photodetector has low dark current [5], [6], very short response time [7]–[11], and process compatibility with high-performance field-effect transistors (FET's) [1], [2], which make it suitable for monolithic integration of optoelectronic circuits.

One of the main challenges for MSM photodetector development is to obtain a short pulse response time without degrading responsivity. In general, the speed of a normal

MSM photodetector is largely limited by the capacitance (RC constant) and by the transit time of the photocarriers traveling across the active region. Fast trapping of photocarriers in proton-implanted regions reduces the response time considerably, unfortunately at the expense of reduced sensitivity. Transit time could be reduced by narrowing the spacing between the contacts, but this increases the capacitance and requires high-resolution electron-beam lithography. A straightforward approach to reduce the capacitance and shorten the response time of the devices is to shrink the active area [12] and to use submicrometer lithography. From the application point of view, however, a large active area is often required, for instance, for interconnects between chips and circuit boards. In order to obtain high response speed, a large bias to the MSM photodetector is preferred since both transit time [13] and capacitance are reduced with increasing bias. However, it is obvious that the bias is limited by the dark current and bias compatibility in a monolithic integrated circuit.

Various MSM photodetector designs using different compromises between the transit time and RC constant [6] have been reported in the literature, with the extreme case being a single gap in a coplanar strip transmission line [14] which showed subpicosecond rise time but very low sensitivity. Although successful in reducing the rise time, most of the designs have yielded a fall time that is typically much longer than the rise time, and this is the limiting factor for high bit rate operation.

In this paper, we report a GaAs/AlGaAs/GaAs sandwich heterostructure MSM photodetector (HMSM) [15]. With this structure, both the transit time and the RC constant are reduced, and the saturation capacitance and the saturation velocity within the entire active region are reached at much lower bias in comparison with a comparable conventional MSM photodetector (CMSM). The fall time and rise time at a bias of 10 V are reduced more than 30% and 20%, respectively. The measured minimum fall time is only 23 ps, which is about the same as the rise time of 30 ps and is the shortest fall time ever reported for an MSM photodetector of $100 \times 100 \mu\text{m}^2$. As this result is close to the rise time of 18 ps of the sampling head used in our measurements, the actual intrinsic response speed could be even higher had the system par-

Manuscript received September 14, 1992; revised January 29, 1993. This work was supported in part by the Ontario Laser and Lightwave Research Center and by the Ontario Center for Material Research. The review of this paper was arranged by Associate Editor J. J. Coleman.

J. Lu is with the Department of Electrical Engineering University of Toronto, Toronto, Ont., Canada M5S 1A4.

R. Surridge and G. Pakulski are with the Advanced Technology Laboratory, Bell-Northern Research Ltd., Ottawa, Ont., Canada K1Y 4H7.

H. van Driel is with the Department of Physics, University of Toronto, Toronto, Ont., Canada M5S 1A4.

J. M. Xu is with the Department of Electrical Engineering, University of Toronto, Toronto, Ont., Canada M5S 1A4, and the Advanced Technology Laboratory, Bell-Northern Research Ltd., Ottawa, Ont., Canada K1Y 4H7.

IEEE Log Number 9208280.

asitics been eliminated by, for instance, the use of electrooptical sampling techniques. As the emphasis of this work is not on establishing the record of absolute speed, but on the comparative advantages of HMSM over CMSM for its response speed and responsivity, the limitation on absolute speed determination is not deemed critical.

Equally important, we show that the peak value of the impulse response of the HMSM is higher than that of the CMSM mainly due to the shorter charging and discharging time, although some of the photocarriers do not contribute because of the heterobarrier in the HMSM. With this design, the tradeoff between response speed and sensitivity is considerably minimized.

II. DEVICE STRUCTURE AND DESIGN CONSIDERATIONS

The basic structure of the HMSM, grown by Molecular Beam Epitaxy (MBE), is shown in Fig. 1. To reduce the transit time of the photocarriers, a wider bandgap material is employed between the active layer and the substrate to prevent the slow and deep photocarriers generated in the substrate from reaching the electrodes. To effectively cut off the deep photocarriers, the thickness of the active layer must be thinner than the absorption depth (about $1.5 \mu\text{m}$ for the incident light with a wavelength of 850 nm in GaAs). This is in contrast with some earlier work where a thick barrier layer was buried several micrometers below the surface to reduce the substrate parasitics [16]. The thickness of the barrier layer must be thick enough to block the slow photocarriers. Taking all these considerations into account, we designed and fabricated the HMSM with a vertical structure consisting of a $1\text{-}\mu\text{m}$ undoped GaAs active layer and a $1\text{-}\mu\text{m}$ $\text{Al}_{0.3}\text{Ga}_{0.7}\text{As}$ barrier layer on an undoped GaAs substrate. The interdigital metal (Ti/Pt/Au) Schottky contacts were formed by using standard bilayer photolithography and a liftoff process. The active area of the device is $100 \times 100 \mu\text{m}^2$. Considering that the saturation velocity of the photocarriers is around $1 \times 10^7 \text{ cm/s}$, wider spacing will result in a longer transit time while a narrower spacing leads to a larger RC constant and higher dark current. A finger width and spacing of 1 and $3 \mu\text{m}$, respectively, were chosen in this work. A CMSM with the same layout was fabricated as a standard for comparison.

III. RESULTS AND DISCUSSION

The optical impulse responses of the HMSM and CMSM at a bias of 10 V are shown in Fig. 2. The optical pulse was generated using a dye laser with a FWHM of 5 ps at a wavelength of 830 nm . The repetition period of the pulse train is 13 ns and the incident optical power is 0.3 mW . The output signal was sent through an HP11612A (26.5 GHz) Bias-T to the SD-26 Sampling Head of a TEK11802 Digital Sampling Oscilloscope, which has a rise time of 18 ps . The measured rise time (10% to 90%) is 32 ps and the fall time (90% to 10%) is 29 ps for the HMSM, while for the CMSM, the rise time is 42 ps and the fall time is 43 ps . The ringing observed

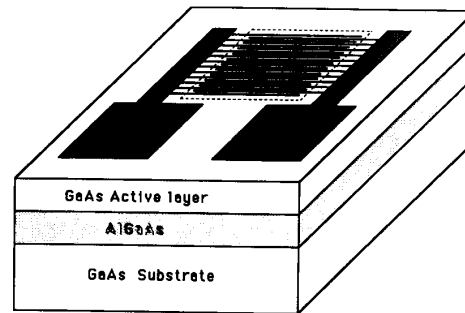


Fig. 1. The basic structure of the HMSM with a $1\text{-}\mu\text{m}$ GaAs active layer, a $1\text{-}\mu\text{m}$ AlGaAs barrier layer, and a GaAs substrate. The shadowed part on the top is contact metal. The area surrounded by the dashed line is the active region.

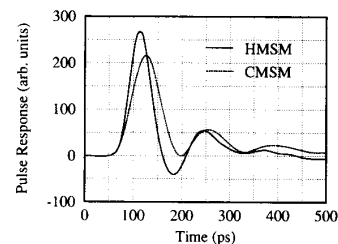


Fig. 2. Pulse response of the HMSM and the CMSM measured at a bias voltage of 10 V .

on the falling edge of the response may be attributed to LC circuit resonance. It is believed to have some effects on quantitative results but not on the main conclusions drawn from our experimental results, according to the SPICE simulations briefly described later in this section.

Fig. 3 shows the rise and fall times of the impulse response as a function of bias voltage. The fall time of the CMSM decreases with increasing bias up to 20 V while the fall time of the HMSM approaches its saturation value at a much lower bias. As can be seen, both the rise time and the fall time of the HMSM are significantly shorter than that of the CMSM within the bias range of $0\text{--}24 \text{ V}$, especially so in the low bias range. This clearly makes HMSM more attractive for applications.

The AlGaAs barrier layer impedes the slow photocarriers generated deep in the substrate, where the electric field is also weak, from being collected by electrodes, leading to a reduced transit time and a suppressed falling tail. Moreover, we find in measurements and calculations that with this AlGaAs barrier the capacitance of HMSM is also reduced substantially. The measured capacitance as a function of applied bias is shown in Fig. 4(a). This displays a similar bias dependence as the fall time versus bias curves shown in Fig. 3(b), indicating that the RC constant is playing a more important role than the transit time in impulse response. The capacitance measurement was carried out by means of an HP8510 network analyzer. A widely used equivalent circuit model for MSM photodetector was employed for extrapolating the parameters. The measured S_{11} parameters under illumination were fit-

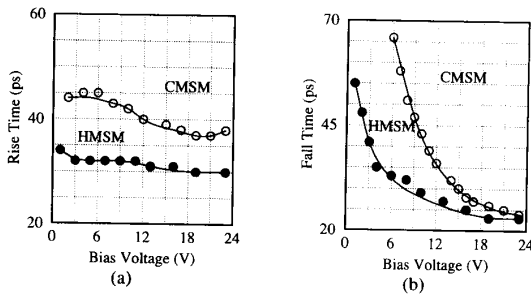


Fig. 3. (a) Rise time of the impulse response versus bias voltage. (b) Fall time of pulse response versus bias voltage.

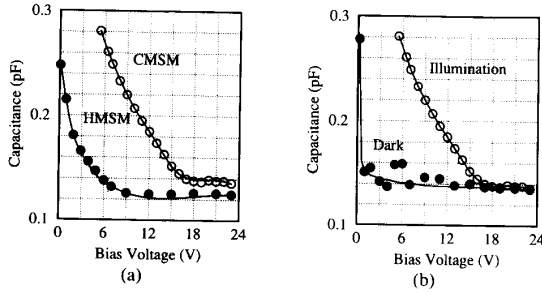


Fig. 4. (a) Capacitance versus bias voltage measured under illumination. (b) Capacitance for the CMSM measured both in the dark and under illumination.

ted by iteratively varying the values of the circuit elements in the frequency range of 0.04 MHz through 26 GHz.

Two physical models commonly used to approximate the capacitance of the MSM photodetector are based on a one-dimensional (1D) approximation [17] or a two-dimensional (2D) conformal mapping technique [18]. For a 1D approximation, when the applied bias V is smaller than the reachthrough voltage V_{RT} , the capacitance of two back-

and (1) reduces to

$$C_{\text{sat}} = \frac{\epsilon_s}{L} \quad (3)$$

Equations (1) and (2) describe the one-dimensional capacitance as a function of the applied bias. Since the practical MSM photodetector is a planar device, as shown in Fig. 1, the field region, in reality, will extend deeper and deeper into the substrate as bias increases, despite the fact that the reachthrough condition is already reached at the surface. A higher saturation bias is therefore expected compared with one-dimensional configuration due to the existence of the weak field region deep in the substrate.

The insertion of the AlGaAs layer in the HMSM provides a nonabsorbing layer which has very low intrinsic carrier concentration, and a barrier which effectively blocks both types of photocarriers in the substrate. Considering that the carrier concentration in the AlGaAs layer could be a few orders of magnitude smaller than that in the GaAs surface layer, the barrier layer can be depleted at a bias even lower than that required to deplete the surface layer. This is supported by our simulation results which will be discussed later. Due to the blocking effect, although the applied field still extends through the barrier to the substrate underneath, the overall net charge in the substrate hardly changes and thus contributes little to the capacitance. Therefore, once the depletion region extends to this barrier layer, the measured capacitance drops to its saturation value. Consequently, we have a lower capacitance and a lower saturation voltage for the HMSM as shown by the lower curve in Fig. 4(a).

Although it predicts the correct trend of capacitance variation with bias, (1) only takes into account the depletion capacitance contributed by charges associated with doping N_D . When the active area is illuminated, the polarization of the photocarriers also contribute to the capacitance unless the electric field is strong enough to

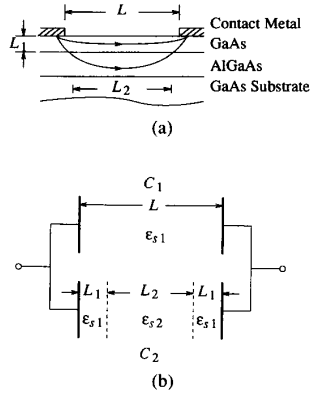


Fig. 5. (a) A cross section of the HMSM photodetector. (b) For a device with a heterostructure depicted in (a), the depletion capacitance could be estimated in terms of the parameters defined in (b). Separating the contributions of the GaAs active layer and the AlGaAs barrier layer to the depletion capacitance, and simplifying them as parallel-plate condensers, yields (b).

by the active layer and C_2 is the capacitance contributed by the barrier layer and $C = C_1 + C_2$. Denoting C_{C2} as C_2 for the CMSM, and C_{H2} for HMSM, we can calculate them, in reference to (3), by

$$C_{C2} = \frac{\epsilon_{s1}}{L_2 + 2L_1} \quad (4)$$

and

$$C_{H2} = \frac{\epsilon_{s1}}{\frac{\epsilon_{s1}}{\epsilon_{s2}} L_2 + 2L_1} \quad (5)$$

where L is the physical spacing between two adjacent electrodes as defined previously, L_1 is the thickness of the active layer, and L_2 is a structure-dependent effective spacing for the capacitance contributed by the barrier layer. ϵ_{s1} and ϵ_{s2} are the dielectric constants for GaAs active layer and AlGaAs barrier layer, respectively. Since $\epsilon_{s1}/\epsilon_{s2} > 1$, C_{H2} will be always smaller than C_{C2} . This is proven by our experimental results, illustrated in Fig. 4(a), and by our two-dimensional simulation which was carried out using our General Purpose Semiconductor Device Analyzer (GPSDA) [19]. Fig. 6 shows that the barrier layer has a very low carrier concentration, and the active layer of the HMSM is thus much more easily depleted than that of the CMSM. It also shows that the carriers in the substrate are effectively blocked from the active layer. The simulated capacitances as a function of bias qualitatively agree with the experimental results. Based on the equivalent circuit for the MSM photodetector and the device parameters extracted from the network analyzer, a transient state simulation of MSM photodetector has been made using SPICE. The simulated fall time as a function of bias is in good agreement with the measured curves in the high-voltage range, while at low bias the simulated fall time is smaller than the experimen-

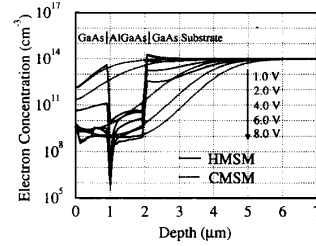


Fig. 6. Electron concentration along the device depth at the middle of the finger gap for both the HMSM (solid lines) and the CMSM (dotted lines) obtained by two-dimensional simulation.

tal results. This is because, at low bias, the photocarriers move at a velocity much lower than their saturation velocity, and therefore the response speed at this point is mainly dependent upon the transit time rather than the RC constant.

Conformal mapping was used to more accurately estimate the depletion capacitance of the MSM photodetector since it takes the 2D effect into consideration. With this approach, the capacitance of the interdigitated MSM photodetector is given by

$$C = \frac{K(k)}{K(k')} \epsilon_0 (1 + \epsilon_r) \quad (6)$$

where $\epsilon_s = \epsilon_0 \epsilon_r$, and $K(k)$ is a complete elliptic integral of the first kind,

$$K(k) \equiv \int_0^{\pi/2} \frac{d\phi}{\sqrt{(1 - k^2 \sin^2 \phi)}}$$

$$k \equiv \tan^2 \frac{\pi}{4} \frac{L}{W + L}$$

$$k' \equiv \sqrt{(1 - k^2)}$$

where W is the finger width, L is as defined above. Here, we should notice that, by taking the two-dimensional effect into account, the width and length of the electrodes contribute to the capacitance differently, unlike the situation in the 1D approximation. The capacitance given by (6) is now the gap capacitance of electrodes per unit length and the contribution of the electrode width is already included in the equation. An assumption of the absence of electrical charge in the system has been made for this approach. Therefore, it could only be used as a good estimation of the device capacitance when the active region of the device is undoped and fully depleted. For a device with the parameters in our device layout, the calculated capacitance by this approach is 0.1 pF, which agrees well with the measured saturation capacitances.

The dependence of the impulse response on the incident light intensity was also investigated in this work within the incident power range of 0.1–10 mW at different bias voltages. As expected, the FWHM of the impulse res-

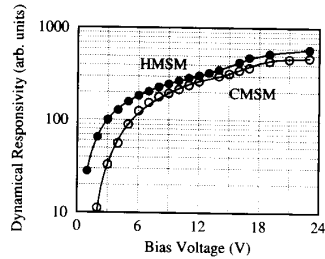


Fig. 7. The dynamic responsivity R_T versus bias voltage.

sponse broadens as the incident light intensity increases due to the contribution of the photoinduced capacitance and longer transit time caused by the weakened electric field as discussed previously.

The incorporation of the AlGaAs barrier layer, by impeding the photocarriers generated deep in the substrate from being collected by the electrodes, causes a reduced dc responsivity. From the application point of view, however, the dc responsivity is not as important as the peak value of the impulse response for a photodetector. For a device which has a smaller capacitance, and in turn a higher charging rate, a higher peak value for a given charging time is expected. The photocarriers which are collected at the electrodes after the photocurrent peak do not contribute as much to the pulse detection, and therefore cutting them off will not reduce the sensitivity of the device. If we take the peak response over incident power as a measure of the responsivity of the photodetector in impulse response, and denote it as the dynamic responsivity R_T , then it is obvious that R_T depends not only on the total number of photocarriers, but also the charging rate. The greater the charging rate, the higher the R_T . Fig. 7 shows the measured dynamic responsivity R_T versus bias voltage, indicating that R_T for the HSM remains higher than that for the CMSM for the range of bias used in the experiment. Based on these results, we can state that the tradeoff between the response speed and the dynamic responsivity can be reduced with the HSM design.

IV. CONCLUSION

Ultrafast MSM photodetectors based on a GaAs/AlGaAs/GaAs heterostructure were studied. This new type of MSM photodetector has a smaller saturation capacitance, in comparison with conventional MSM photodetectors, and is able to reach this value at a much lower bias, both in the dark and under illumination. The measured fall time is 29 ps at a bias of 10 V, and the minimum fall time is only 23 ps for an HSM photodetector with a moderate active area of $100 \times 100 \mu\text{m}^2$. The peak value of the impulse response for the HSM remains higher than that for the CMSM within the whole range of test bias voltage from 0–24 V. With this structure, both the transit time and the RC constant are reduced. Moreover, the response speed is improved without degrading the sensitivity of the temporal response. This type of MSM

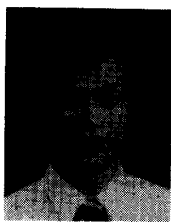
photodetector provides a new alternative in obtaining an optimized MSM technology.

ACKNOWLEDGMENT

The authors wish to thank G. L. Tan and Q. M. Zhang for their help in two-dimensional simulation, and also K. Lee for helpful discussions.

REFERENCES

- [1] M. Ito, O. Wada, K. Nakai, and T. Sakurai, "Monolithic integration of a metal-semiconductor-metal photodiode and a GaAs preamplifier," *IEEE Electron Device Lett.*, vol. EDL-5, pp. 531–532, Dec. 1984.
- [2] D. L. Rogers, "Monolithic integration of a 3-GHz detector/preamplifier using a refractory-gate, ion-implanted MESFET process," *IEEE Electron Device Lett.*, vol. EDL-7, pp. 600–602, Nov. 1986.
- [3] H. Hamaguchi, M. Makiuchi, T. Kumai, and O. Wada, "GaAs optoelectronic integrated receiver with high-output fast-response characteristics," *IEEE Electron Device Lett.*, vol. EDL-8, pp. 39–41, Jan. 1987.
- [4] C. S. Harder, B. Van Zeghbroeck, H. Meier, W. Patrick, and P. Vettiger, "5.2-GHz bandwidth monolithic GaAs optoelectronic receiver," *IEEE Electron Device Lett.*, vol. 9, pp. 171–173, Apr. 1988.
- [5] M. Ito and O. Wada, "Low dark current GaAs metal-semiconductor-metal (MSM) photodetector using WSi₂ contacts," *IEEE J. Quantum Electron.*, vol. QE-22, pp. 1073–1077, July 1986.
- [6] D. S. Malhi, J. M. Xu, F. Hegmann, B. Takasaki, and R. Surridge, "Effects of material modification on dark current of GaAs MSM photodetectors," in *Semi-Insulating III-V Materials*, A. G. Milnes and C. J. Miner, Eds. Philadelphia, PA, Toronto, Canada: Hegler, 1990, pp. 451–456.
- [7] W. Roth, H. Schumacher, J. Kluge, H. J. Geelen, and H. Beneking, "The DSI diode—A fast large-area optoelectronic detector," *IEEE Trans. Electron Devices*, vol. ED-32, pp. 1034–1036, June 1985.
- [8] W. S. Lee, G. R. Adams, J. Mun, and J. Smith, "Monolithic GaAs photoreceiver for high speed signal processing applications," *Electron. Lett.*, vol. 22, pp. 147–148, Jan. 1986.
- [9] B. J. Van Zeghbroeck, W. Patrick, J. M. Halbout, and P. Vettiger, "105-GHz bandwidth metal-semiconductor-metal photodiode," *IEEE Electron Device Lett.*, vol. 9, pp. 527–529, Oct. 1988.
- [10] C. Mogilestue, J. Rosenzweig, J. Kuhl, M. Klingenstein, M. Lambsdoff, A. Axmann, J. Schneider, and A. Hulsmann, "Picosecond pulse response characteristics of GaAs metal-semiconductor-metal photodetectors," *J. Appl. Phys.*, vol. 70, no. 4, pp. 2435–2448, Aug. 1991.
- [11] Y. Chen, S. L. Williamson, T. Brock, and F. W. Smith, "1.9 picosecond optical temporal analyzer using 1.2 picosecond photodetector and gate," in *IEDM Tech. Dig.* (Washington, DC), 1991, pp. 417–420.
- [12] M. Klingenstein and J. Kuhl, "Transit time limited response of GaAs metal-semiconductor-metal photodiodes," *Appl. Phys. Lett.*, vol. 58, pp. 2503–2505, June 1991.
- [13] J. B. D. Soole and H. Schumacher, "InGaAs metal-semiconductor-metal photodetectors for long wavelength optical communications," *IEEE J. Quantum Electron.*, vol. 27, pp. 737–752, Mar. 1991.
- [14] G. A. Mourou and K. E. Meyer, "Subpicosecond electro-optic sampling using coplanar strip transmission lines," *Appl. Phys. Lett.*, vol. 45, pp. 492–494, 1984.
- [15] L. Figueroa and C. W. Slayman, "A novel heterostructure interdigital photodetector (HIP) with picosecond optical response," *IEEE Electron Device Lett.*, vol. EDL-2, pp. 208–210, Aug. 1981.
- [16] R. K. Surridge and J. M. Xu, "MSM photodetector with superlattice," U.S. Patent, 4 998 154, 1990.
- [17] S. M. Sze, D. J. Coleman, Jr., and A. Loya, "Current transport in metal-semiconductor-metal (MSM) structures," *Solid-State Electron.*, vol. 14, pp. 1209–1218, 1971.
- [18] Y. C. Lim and R. A. Moore, "Properties of alternately charged coplanar parallel strip by conformal mappings," *IEEE Trans. Electron Devices*, vol. ED-15, pp. 173–180, Mar. 1968.
- [19] G. L. Tan, Q. M. Zhang, and J. M. Xu, "Computation of field and charge transport in compound semiconductor devices—Some new features and methods," *IEEE Trans. Magn.*, vol. 27, no. 5, pp. 4158–4161, Sept. 1991.



Jian Lu was born in P. R. China in 1958. He received the B.E. degree in electronics engineering from Xian Jiaotong University, P. R. China, in 1982.

He joined the Shanghai Institute of Technical Physics, Chinese Academy of Science, where he worked on the studies of II-VI compound semiconductor heterostructure growth by means of molecular beam epitaxy and the infrared photo-detector array. Since 1990, he has been working towards the M.A.Sc. degree at the University of Toronto, Toronto, Ont., Canada. In 1992, he joined ITS Electronics Inc., Canada, as a member of technical staff. His current research interests include high-speed optoelectronic devices and the integrated circuit (OEIC), the monolithic microwave integrated circuit (MMIC), as well as optical links.

R. Surridge, photograph and biography not available at the time of publication.

G. Pakulski, photograph and biography not available at the time of publication.



Henry M. van Driel was born in Breda, The Netherlands, in 1946. He received the B.S., M.S., and Ph.D. degrees in physics from the University of Toronto, Toronto, Ont., Canada, in 1970, 1971, and 1975, respectively.

During 1975-1976 he was a National Research Council of Canada Post-doctoral Fellow at the Optical Sciences Center, University of Arizona, Tucson. Since 1976 he has been on the Faculty of the University of Toronto, where he is currently Professor of Physics. He has also been a visiting

scientist at Harvard University, IBM T. J. Watson Research Center, and the Max Planck Institut für Festkörperforschung. His present interests are in the development of femtosecond optical parametric sources, the interaction of ultrashort laser pulses with semiconductors, and nonlinear optics at solid surfaces. He is the recipient of a J. S. Guggenheim Fellowship (USA) and an Alexander von Humboldt Award (Germany).

Dr. van Driel is a member of the Canadian Association of Physicists and the American Physical Society; he is a Fellow of the Optical Society of America.



J. M. Xu (M'87-SM'91) received the Ph.D. degree in electrical engineering from the University of Minnesota, Minneapolis, in 1987.

He joined the faculty of the Department of Engineering at the University of Toronto, Toronto, Ont., Canada, in 1987. He is now the J. M. Ham Chair Professor in Optoelectronics, jointly sponsored by the Natural Sciences and Engineering Research Council of Canada and by Bell-Northern Research Ltd. He has authored and co-authored over 70 referred papers in physics and engineering journals, and over 30 refereed conference papers. He holds seven patents on electronic and photonic devices. His current research interests include semiconductor physics, nanostructures, as well as compound semiconductor device design, modeling, and measurements. Currently, he leads a group of 14 researchers and graduate students of the Optoelectronics Laboratory at the University of Toronto and conducts research primarily in the areas of heterostructure transistors, quantum-well devices, lasers, waveguiding devices, and other optoelectronic devices, as well as large-scale computer simulations. The Optoelectronics Laboratory is sponsored by Bell-Northern Research Ltd. through the BNR-NSERC Chair program. He is a principal investigator of the Ontario Laser and Lightwave Research Centre. He is also an Investigator of the Ontario Centre for Materials Research and a Key Associate of the Information Technology Research Centre. He has served on a number of conference program committees.

Dr. Xu is an Associate Editor of IEEE TRANSACTIONS ON ELECTRON DEVICES.